Published Online: 2025 October 1

Research Article

Unveiling the Bioactive Potential of *Allium colchicifolium* Boiss Bulb Flavonoids: Anti-cancer Activities, and Computational Exploration of Anti-angiogenic Mechanisms

Mohammad Bagher Majnooni [1], Mustafa Ghanadian [2,*], Kamran Mansouri [3], Golam Reza Bahrami [1], Mahdi Mojarrab [1,**]

[1] Pharmaceutical Sciences Research Center, Health Institute, Kermanshah University of Medical Sciences, Kermanshah, Iran
[2] Department of Pharmacognosy, Isfahan Pharmaceutical Sciences Research Center, School of Pharmacy and Pharmaceutical Sciences, Isfahan University of Medical Sciences, Isfahan, Iran
[3] Medical Biology Research Center, Health Technology Institute, Kermanshah University of Medical Sciences, Kermanshah, Iran

[*] ***Corresponding Author:*** Department of Pharmacognosy, Isfahan Pharmaceutical Sciences Research Center, School of Pharmacy and Pharmaceutical Sciences, Isfahan University of Medical Sciences, Isfahan, Iran. Email: ghannadian@gmail.com
[**] ***Corresponding Author:*** Pharmaceutical Sciences Research Center, Health Institute, Kermanshah University of Medical Sciences, Kermanshah, Iran. Email: mahdi.mojarab@gmail.com

Received: 24 May, 2025; **Revised:** 8 September, 2025; **Accepted:** 20 September, 2025

Abstract

Background: Plants of the genus *Allium* show significant anti-cancer properties due to various phytochemicals, including flavonoids.

Objectives: This study investigated the cytotoxic activities of the methanolic extract of *Allium colchicifolium* bulbs and its purified flavonoids. It also assessed the anti-angiogenic activities, a key mechanism of anti-cancer agents.

Methods: The methanolic extract was fractionated using column chromatography (CC) on silica gel RP-18 and polyamide SC-6, then purified with Sephadex LH-20. The compounds were identified through spectroscopic methods such as nuclear magnetic resonance (NMR) and liquid chromatography-electrospray ionization-tandem mass spectrometry (LC-ESI-MS/MS). Cytotoxicity and anti-angiogenic activities were evaluated using the MTT assay and the chick chorioallantoic membrane (CAM) assay, respectively. Computational modeling explored the potential anti-angiogenic mechanisms of the purified compounds. Additionally, absorption, distribution, metabolism, excretion, and toxicity (ADMET) profiling predicted drug-likeness features.

Results: Three flavonoids — quercetin 3-O-rutinoside (1), isorhamnetin 3-O-glucoside (2), and quercetin (3) — were isolated and identified. Compounds 2 and 3 showed the highest cytotoxicity against PC3 (prostate cancer, $IC_{50} = 1.72 \pm 0.11$ μg/mL) and MCF-7 (breast cancer, $IC_{50} = 1.64 \pm 0.11$ μg/mL) cell lines. The methanolic extract and compound 3 also had potent anti-angiogenic effects with IC_{50} values of 4.2 ± 0.25 and 5.3 ± 0.3 μg/mL, respectively. Molecular docking indicated that compounds 1 and 3 had the strongest interactions with the vascular endothelial growth factor receptor (VEGFR)-1, consistent with their anti-angiogenic activity. The ADMET profiling showed that compound 3 had the highest similarity to drug-like molecules.

Conclusions: This was the first phytochemical study of flavonoids in *A. colchicifolium* bulbs. The results suggest that these bulbs could serve as a natural source for cancer prevention and treatment, owing to their cytotoxic and anti-angiogenic properties. Further research is needed to confirm these findings, and in vivo studies are essential to validate their therapeutic potential.

Keywords: *Allium colchicifolium*, Phytochemical Study, Flavonoids, Cytotoxicity, Anti-angiogenesis, VEGF, Column Chromatography, Molecular Docking

1. Background

Flavonoids are a key group of polyphenolic compounds characterized by a C6-C3-C6 carbon structure, and their anti-cancer properties have long been a focus of research (1). Flavonoids prevent the proliferation and growth of cancer cells by blocking cellular signaling pathways involved in apoptosis and cell cycle regulation, such as mitogen-activated protein kinases (MAPK), phosphoinositide 3-kinase (PI3K)/protein kinase B (AKT)/mammalian target of rapamycin (mTOR), nuclear factor-kB (NF-kB), Janus kinases (JAK)/signal transducer and activator of transcription (JAK/STAT3), among others (1-3). Additionally, flavonoids exhibit prominent anti-angiogenic effects by inhibiting the expression of genes that mediate angiogenesis, including vascular endothelial growth factor (VEGF) and hypoxia-inducible

How to Cite: Majnooni M B, Ghanadian M, Mansouri K, Bahrami G R, Mojarrab M. Unveiling the Bioactive Potential of *Allium colchicifolium* Boiss Bulb Flavonoids: Anti-cancer Activities, and Computational Exploration of Anti-angiogenic Mechanisms. Iran J Pharm Res. 2025; 24 (1): e163152. https://doi.org/10.5812/ijpr-163152.

factor-1 alpha (HIF-1α), thereby preventing tumor growth and metastasis (4). Clinical studies have shown that flavonoids improve the likelihood of treating various cancers. Besides impacting the proliferation, growth, migration, and metastasis of tumor cells, these compounds also increase the cells' sensitivity to chemotherapy and help reduce drug resistance (1, 5).

Allium species (Amaryllidaceae), including *Allium flavum* (1), *A. ascalonicum* (2), *A. cepa* (3), *A. sativum*, and *A. fistulosum* (4), exhibit prominent anti-cancer and anti-angiogenic activities due to their diverse secondary metabolites. These include flavonoids such as quercetin and kaempferol, as well as organosulfur compounds like diallyl thiosulfinate (allicin) and diallyl sulfides (5-7). Abdel-Hady et al. demonstrated that a kaempferol derivatives-rich extract of *A. kurrat* exhibited cytotoxic activities against colon and liver cancer cell lines (8). Additionally, a quercetin-rich fraction from *A. cepa* revealed cytotoxic activities against adrenal carcinoma cell lines (3). A flavonoid-rich extract of *A. hirtifolium* prevented vessel growth in various in vitro angiogenesis models by blocking VEGF gene expression (9). An in vivo study on *A. flavum* and *A. carinatum* extracts exhibited that these high-flavonoid extracts, both alone and in combination with the broad-spectrum chemotherapeutic drug doxorubicin, significantly inhibited angiogenesis (10).

The promising anticancer effects of flavonoids such as hesperidin, quercetin, apigenin, and luteolin, and their glycosylated derivatives, have led to the design and implementation of numerous clinical trials across various phases for these compounds (11).

Allium colchicifolium (synonym: *A. bischoffii* Hausskn. ex Dinsm) is one of the *Allium* species native to western Iran, particularly the mountains of Kermanshah province. This plant was first documented by Wendelbo in 1971 on Bisotun Mountain, east of Kermanshah, Iran (12, 13). In folk medicine, *A. colchicifolium* is used to treat rheumatoid arthritis, joint pain, cholesterolemia, and inflammation. It is also used to prepare several local foods (14, 15).

2. Objectives

Based on this evidence, the present study purified flavonoids from the methanol (MeOH) extract of *A. colchicifolium* bulbs and identified them using one-dimensional and two-dimensional nuclear magnetic resonance (NMR) spectroscopy and liquid chromatography-electrospray ionization-tandem mass spectrometry (LC-ESI-MS/MS). We also evaluated the cytotoxic and anti-angiogenic activities of the extract and its isolated flavonoids.

3. Methods

3.1. General Experimental Procedures

A Bruker Avance AV 400 ^{1}H NMR [400 MHz, DMSO-d6 (99.9% purity, Mesbah Energy, Iran)] and ^{13}C NMR [100 MHz, DMSO-d6 (99.9% purity, Mesbah Energy, Iran)] were used to record NMR spectra. The heteronuclear multiple bond correlation (HMBC) NMR was used to determine two and three-bond heteronuclear ^{1}H-^{13}C connectivity. An Agilent LC (1200 series, Germany)-ESI-MS/MS (Agilent Technologies, Palo Alto, CA, USA) was used for molecular ion mass analysis. The column chromatography (CC) was run on polyamide-SC6 (Roth, Germany) and Sephadex-LH (Pharmacia Fine Chemicals, Sweden) and eluted with gradient solvent systems, chloroform ($CHCl_3$): MeOH (Merck, Germany). Thin-layer chromatography (TLC) was run on TLC silica gel (SiO_2, Merck, Germany) with $CHCl_3$: MeOH 9:1. 1% natural product reagent (NP, 2-aminoethyl diphenylborinate, Merck, Germany) was used to visualize polyphenol spots on TLC. All statistical analyses were performed using SPSS software version 23.0 and Excel 2016.

3.2. Plant Material

Allium colchicifolium was gathered from Mian Rehan (34°35′02″N 47°26′34″E) in Kermanshah province, western Iran, during the flowering period from April to May by local herbal collectors trained by herbarium experts at the Kermanshah Faculty of Pharmacy. This plant was confirmed by comparison with the voucher specimen (No. 001-036-001-160) available in the herbarium of the Pharmacognosy Department, Faculty of Pharmacy, Kermanshah University of Medical Sciences (16).

3.3. Extraction and Isolation

The *A. colchicifolium* dried bulbs (350 g) were ground and extracted sequentially with hexane, $CHCl_3$, $CHCl_3$/MeOH (9:1), and MeOH solvents (1.5 L each, for 3 days) at room temperature using the method described by Fattorusso et al. (17). All extracts were filtered through

Whatman No. 1 filter paper and concentrated with a rotary evaporator (50°C, 70 mbar). The MeOH extract (10 g) was chromatographed on a silica gel RP-18 column (3 × 30 cm) using a gradient solvent system from H_2O to MeOH (100 → 0) to yield 10 fractions (Fr.1-Fr.10). The TLC profile (SiO_2, $CHCl_3$: MeOH, 9:1) of Fr.5 (H_2O: MeOH, 50:50) and Fr.6 (H_2O: MeOH, 40:60) showed most yellow spots after spraying the NP and were selected as rich-polyphenol fractions. Fr.5 and Fr.6 were re-chromatographed on a polyamide SC6 column (3 × 40 cm) using a linear gradient solvent system from $CHCl_3$ to MeOH (95:5, 90:10, 85:15, 80:20, 70:30, each 500 mL). According to the TLC profile, Fr.5f ($CHCl_3$ to MeOH 70:30), Fr.6c ($CHCl_3$ to MeOH 85:15), and Fr.6d ($CHCl_3$ to MeOH 80:20) were selected for the next steps. Fr.5f was chromatographed on a Sephadex LH-20 column (3 × 80 cm; MeOH) to yield Fr.5f1 and Fr.5f2. Fr.5f1 was obtained in a pure state as compound 1 (8 mg, Rf = 0.22). Fr.6c and Fr.6d were re-chromatographed under the same column conditions to yield compound 2 (9 mg, Rf = 0.3) and compound 3 (11 mg, Rf = 0.55), respectively.

3.4. Cytotoxicity Activities

3.4.1. Cell Lines and Culture

Cancer cell lines, including PC3 NCBI-C427 (human prostate adenocarcinoma), HeLa NCBI-C115 (human cervix carcinoma), MCF7 NCBI-C135 (human breast adenocarcinoma), and a normal cell line, human umbilical vein endothelial cell (HUVEC) NCBI-C554, were purchased from the Pasteur Institute of Tehran, Iran. Cells were cultured and maintained in Dulbecco's modified Eagle's medium (DMEM) supplemented with 10% fetal bovine serum (FBS) and 2% (v/v) streptomycin-penicillin in a humidified incubator with a 5% CO_2 atmosphere at 37°C. Passages 2 to 3 of the cells were utilized for the cytotoxicity assay (18).

3.4.2. MTT Assay

The MTT assay was used to determine the cytotoxic activities of the MeOH extract, isolated compounds (1 - 3), and doxorubicin (as a positive control) on human cancer cell lines. For the MTT assay, concentrations (1, 5, 10, 25, 50, 100 µg) of the samples were prepared in DMEM as diluent and incubated with cells (10^5 cells/mL) for 24 hours in 96-well plates. Then, the MTT powder was added to the wells and incubated for 4 hours at 37°C. Absorbance was measured at 570 nm using a microplate reader. The experiment was performed in triplicate, and cell viability percentages were calculated by the following equation: % Cell viability = [(OD negative control - OD tested compounds)/(OD negative control)] × 100. The negative control was untreated cells. The cytotoxicity IC_{50} value for the extracts was defined as the concentration that reduces 50% cell viability (19).

3.5. Anti-angiogenic Activities

The anti-angiogenesis activities of the MeOH extract and isolated compounds (1-3) were evaluated using the chicken chorioallantoic membrane (CAM) model. Briefly, pathogen-free fertilized chicken eggs were purchased from Baharan Parent Stock Company, Kermanshah, Iran, and incubated at 37°C with 75% humidity for 7 days. Then, square windows (1 cm^2) were opened in the outer shell of the eggs, and different concentrations of samples were loaded. After 48 hours, the zones around the discs were photographed with a digital camera and macroscopically assayed for neovascular zones of CAM in each treatment group. The effects on local vessel density within a 10 cm^2 area surrounding the windows were measured in each treatment group using AngioSoft software (V, 2019) (12, 13). The study was done in triplicate for each experimental group (8 eggs). The anti-angiogenesis IC_{50} value for the extracts was reported as the concentration that reduces 50% angiogenesis compared to the blank disk.

3.6. Molecular Docking

Crystal structures of the target proteins, VEGF-R1 [Protein Data Bank (PDB) ID: 3HNG]; VEGF-A (PDB ID: 1VPF), VEGF-B (PDB ID: 2C7W), VEGF-C (PDB ID: 2X1X), VEGF-D (PDB ID: 2XV7) were downloaded from the PDB (http://www.RCSB.org). The co-crystallized ligands, cofactors, and water molecules were deleted. Afterwards, hydrogen atoms were added and Gasteiger charges were assigned using Chimera 1.13 (14). Ligand structures generated by ACDLabs ChemSketch (freeware, 2015 2.5) (15) were prepared by adding hydrogens, Gasteiger charges, and energy minimization through Chimera 1.13. The active site of vascular endothelial growth factor receptor (VEGFR)-1 (PDB ID: 3HNG) was identified from its co-crystallographic

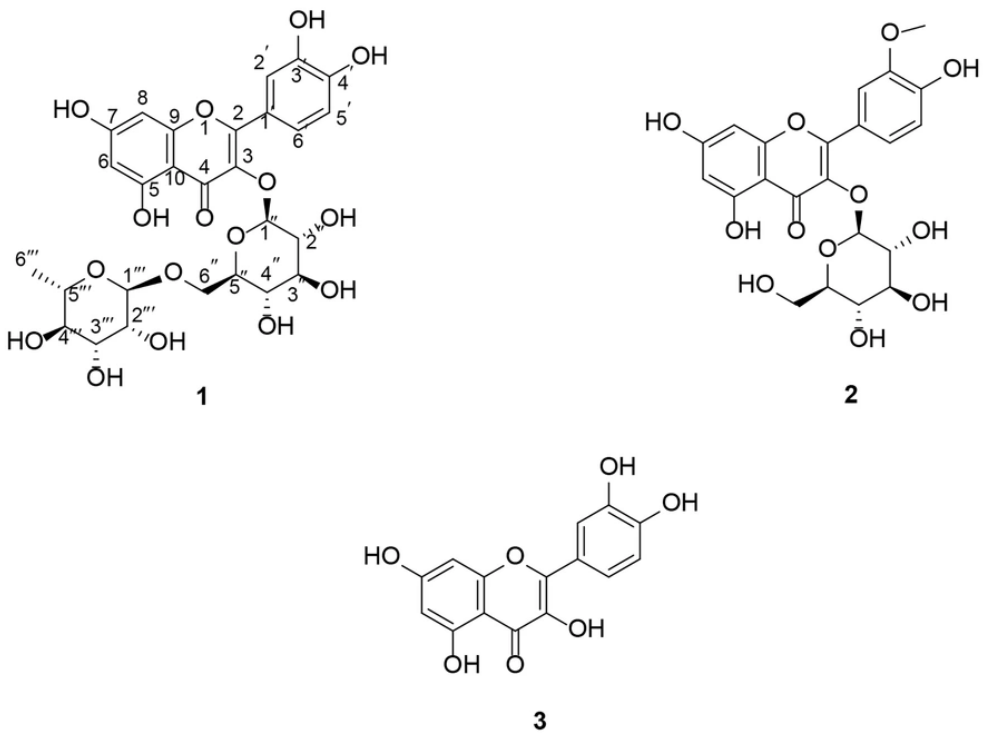

Figure 1. Chemical structure of flavonoids isolated from *Allium colchicifolium* bulbs

ligand. For recognizing binding sites of VEGF-A, VEGF-B, and VEGF-D, the Computed Atlas of Surface Topography of Proteins (CASTp) server (http://sts.bioe.uic.edu/castp/) was utilized (20). In the case of VEGF-C (PDB ID: 2X1X), several residues at the interface of VEGF-C and VEGFR-2 were selected as the binding site (21). Molecular docking was conducted by Autodock Vina in PyRx 0.8 software with exhaustiveness of 50 for each target protein. The grid box dimensions for VEGFR-1 and VEGFR-2 were determined to be 28.41 × 28.02 × 27.79 Å and 28.25 × 25.00 × 22.20 Å, respectively, to cover the binding sites (22). Then, LigPlot^{+} (V 2.2) was used to analyze the type of interactions between protein and ligand (23).

3.7. Absorption, Distribution, Metabolism, Excretion, and Toxicity Analysis

The success of a drug is dependent on an acceptable absorption, distribution, metabolism, excretion, and toxicity (ADMET) profile in addition to the good efficacy of the drug (24). In this study, the physicochemical properties of three compounds were extracted using the ADMETlab 2.0 web tool, and Lipinski's Rule of 5 (Ro5) was used for evaluating drug-likeness (25). Moreover, pharmacokinetic parameters and toxicity of these compounds were predicted by the AdmetSAR database (http://lmmd.ecust.edu.cn/admetsar1/).

4. Results and Discussion

4.1. Isolation and Identification of Compounds

Plants and their active compounds have long been of interest to researchers for cancer treatment. In this study, we investigated the phytochemical profile of *A. colchicifolium* bulbs along with their cytotoxic and anti-angiogenic activities. The *A. colchicifolium* dried bulbs (350 g) were successfully extracted with hexane, $CHCl_3$, $CHCl_3$: MeOH (9:1), and MeOH solvents, with yields of 3.5 g (1%), 5.6 g (1.6%), 17.5 g (5%), and 14.7 g (4.2%), respectively. MeOH was fractionated and purified using CC on RP-18, SC6 polyamide, and Sephadex LH-20, which

yielded seven fractions and three purified flavonoids (Figure 1), including quercetin 3-O-rutinoside (compound 1), isorhamnetin 3-O-glucoside (compound 2), and quercetin (compound 3).

Based on the LC-MS/MS analysis in negative mode and collision energy 15 eV, compound (1) exhibited a molecular ion $[M-H]^-$ at 609 m/z. The results of fragmentation of 609 m/z showed 463 m/z, 301 m/z, 273 m/z, and 151 m/z, which corresponded to a glycosylated flavonoid (Appendix 1 in Supplementary File) (26, 27). Additionally, the ^{1}H NMR spectra of (1) showed five protons in the aromatic region at δH 6.19 (1H, d, J = 2.1 Hz, H-6), 6.38 (1H, d, J = 2.1 Hz, H-8), 6.92 (1H, d, J = 8.48 Hz, H-5′), 6.84 (1H, d, J = 8.3 Hz, H-5′), 7.53 (1H, d, J = 2.3 Hz, H-2′), 7.55 (1H, dd, J = 8.3, 2.3 Hz, H-6′). Also, two signals at δH 5.4 (1H, d, J = 7.30 Hz, H-1″) and 4.45 (1H, bs, H-1‴) corresponded to anomeric protons of glucose and rhamnose, respectively. Protons of glucosyl H-2″-H-6″ and rhamnosyl H-2‴-H-5‴ overlapped at 3.12-5.2 ppm, and rhamnosyl H-6‴ appeared at 1.11 (1H, d, J = 6.4 Hz). The signals of OH groups appeared at δH 12.66 (1H, s, 5-OH), 10.91 (1H, s, 7-OH), 9.75 (1H, s, 3′-OH), and 9.26 (1H, s, 4′-OH). Besides, the ^{13}C NMR of compound (1) showed 27 carbon signals. The signals at δc 100.72 and 101.13 corresponded to the anomeric carbon of rhamnose and glucose, respectively. The carbon signal of C-6‴ and C-4 (carbonyl group) appeared at δc 17.79 and 177.32.

Additionally, the HMBC analysis revealed the correlation between the H anomeric of glucose with C-3 and the H anomeric of rhamnose with H-6″. Other HMBC analysis results were depicted in Appendix 2 in Supplementary File. According to the aforementioned information, compound 1 was identified as quercetin 3-O-rutinoside (rutin). Rutin was isolated from *A. cepa* and several other *Allium* species (7, 28, 29).

The results of fragmentation of compound 2 by LC-MS/MS showed the molecular ions at $[M-H]^-$ 477 m/z, [M-H-Glu] 314 and 315 m/z, [315-OH] 299 m/z, [315-OCH_3] 284 m/z, [299-CO] 271 m/z, and [284-$C_8H_6O_2$] 151 m/z, which confirmed a methoxy glucosylated flavonoid structure for compound 2 (26, 27). On the other hand, the presence of five protons in aromatic regions (δH 6 - 8 ppm), a signal at δH 3.85 (3H, s, 3′-OCH_3), a doublet signal corresponding to the anomeric H of glucose at δH 5.58 (1H, d, J = 7.26 Hz), and the presence of 22 carbons in ^{13}C NMR analysis confirmed the isorhamnetin 3-O-glucoside structure for compound 2 (30). *Allium* macrostemon and A. neapolitanum are other sources of isorhamnetin 3-O-glucoside (31, 32). Also, our team isolated isorhamnetin 3-O-glucoside from leaves of *A. colchicifolium* in a parallel study (16).

Based on the LC-MS/MS analysis in negative mode, compound 3 showed a molecular ion $[M-H]^-$ at 301 m/z. The fragmentation results of 301 m/z produced [M-H-CH_3] 284 m/z, [M-H-CO] 271 m/z, [M-H-CH_3-CO] 255 m/z, and [M-H-CH_3-$C_8H_6O_2$] 151 m/z, confirming the flavonoid structure of compound 3. Also, the ^{1}H NMR and ^{13}C NMR spectra of compound 3 corresponded to quercetin isolated from *A. colchicifolium* leaves in our previous study, so compound 3 was identified as quercetin (20).

Compound 1: Yellow powder, ^{1}H-NMR in DMSO-d6 (400 MHz) ppm, δH: 1.11 (1H, d, J = 6.4 Hz, H-6‴), 3.12-5.2 (overlapped, H-2″-H-6″ and H-2‴-H-5‴), 4.45 (1H, bs, H-1‴), 5.4 (1H, d, J = 7.30 Hz, H-1″), 6.19 (1H, d, J = 2.1 Hz, H-6), 6.38 (1H, d, J = 2.1 Hz, H-8), 6.92 (1H, d, J = 8.48 Hz, H-5′), 6.84 (1H, d, J = 8.3 Hz, H-5′), 7.53 (1H, d, J = 2.3 Hz, H-2′), 7.55 (1H, dd, J = 8.3, 2.3 Hz, H-6′), 9.26 (1H, s, 4′-OH), 9.75 (1H, s, 3′-OH), 10.91 (1H, s, 7-OH), 12.67 (1H, s, 5-OH); ^{13}C-NMR (100 MHz, DMSO-d6) δc: 177.32 (C-4), 164.04 (C-7), 161.19 (C-5), 156.59 (C-2), 156.52 (C-9), 148.38 (C-3′), 144.72 (C-4′), 133.26 (C-3), 121.56 (C-6′), 121.13 (C-1′), 116.15 (C-5′), 115.19 (C-2′), 103.93 (C-10), 101.13 (C-1″), 100.72 (C-1‴), 98.64 (C-6), 93.56 (C-8), 76.39 (C-3″), 75.86 (C-5″), 74.03 (C-2″), 71.79 (C-4‴), 70.51 (C-3‴), 70.33 (C-2‴), 69.95 (C-4″), 68.21 (C-5‴), 66.96 (C-6″), 17.79 (C-6‴). Negative ESI mass (m/z): (M-H) – 609, 463, 301, 285, and 150.9.

Compound 2: Yellow powder, ^{1}H-NMR in DMSO-d6 (400 MHz) ppm, δH: 3.11 - 3.58 (overlapped, H-2″- H-6″), 3.85 (3H, s, 3′-OCH_3), 5.58 (1H, d, J = 7.10, H-1″), 6.21 (1H, d, J = 2.14, H-6), 6.42 (1H, d, J = 2.14, H-8), 6.92 (1H, d, J = 8.37, H-5′), 7.50 (1H, dd, J = 8.37, 2.05, H-6′), 7.95 (1H, d, J = 2.05, H-2′), 9.89 (1H, s, 4′-OH), 12.61 (1H, s, 5-OH); ^{13}C-NMR (100 MHz, DMSO-d6) δc: 177.35 (C-4), 164.57 (C-7), 161.19 (C-5), 156.40 (C-2), 156.21 (C-9), 149.37 (C-3′), 146.85 (C-4′), 132.89 (C-3), 121.99 (C-6′), 121.04 (C-1′), 115.17 (C-5′), 113.42 (C-2′), 103.91 (C-10), 100.72 (C-1″), 98.76 (C-6), 93.71 (C-8), 77.41 (C-5″), 76.36 (C-3″), 74.30 (C-2″), 69.75 (C-4″), 60.53 (C-6″), and 55.61 (3′–OCH_3). Negative ESI mass (m/z): (M-H) – 477, 315, 314, 299, 284, 271, and 151.

Compound 3: Pale yellow powder, ^{1}H-NMR in DMSO-d6 (400 MHz) ppm, δH: 6.20 (1H, d, J = 1.75 Hz, H-6), 6.43 (1H, d, J = 1.75 Hz, H-8), 6.91 (1H, d, J = 9.92 Hz, H-5′), 7.56

Table 1. Cytotoxic Activities of Isolated Compounds (1-3) and MeOH Extract of *Allium colchicifolium* Bulbs [a, b]

Variables	PC3	MCF-7	HeLa	HUVEC
Compound 1	2.96 ± 0.16	3.16 ± 0.3	6.95 ± 0.32	9.35 ± 0.8
Compound 2	1.72 ± 0.02 [c]	2.58 ± 0.21	8.43 ± 0.32	9.96 ± 0.37
Compound 3	3.11 ± 0.1	1.64 ± 0.11 [d]	6.17 ± 0.13 [e]	7.23 ± 0.29 [f]
MeOH extract	2.16 ± 0.02 [c]	1.84 ± 0.06 [d]	5.39 ± 0.33 [e]	6.83 ± 0.21 [f]
Doxorubicin	0.051 ± 0.004 [g]	0.034 ± 0.01 [g]	0.066 ± 0.007 [g]	0.045 ± 0.006 [g]

Abbreviation: HUVEC, human umbilical vein endothelial cell.

[a] Values are expressed as IC_{50} (µg/mL) and mean ± SD.

[b] The results of the cytotoxic activity of each compound were compared with the other compounds, and the statistical power was calculated to be 95%.

[c] Significant difference in cytotoxic activities on PC3 (post-hoc Tukey, $P < 0.01$).

[d] Significant difference in cytotoxic activities on MCF-7 (post-hoc Tukey, $P < 0.01$).

[e] Significant difference in cytotoxic activities on HeLa (post-hoc Tukey, $P < 0.01$).

[f] Significant difference in cytotoxic activities on HUVEC (post-hoc Tukey, $P < 0.01$).

[g] Significant difference in cytotoxic activities on the study cell lines (post-hoc Tukey, $P < 0.001$).

(1H, dd, J = 9.92, 1.7 Hz, H-6′), 7.70 (1H, d, J = 1.7 Hz, H-2′), 12.52 (1H, bs, 5-OH); ^{13}C-NMR (100 MHz, DMSO-d6) δc: 175.52 (C-4), 164.45 (C-7), 160.45 (C-5), 156.15 (C-9), 147.77 (C-4′), 146.65 (C-2), 145.09 (C-3′), 135.64 (C-3), 121.88 (C-6′), 119.92 (C-1′), 115.61 (C-5′), 115.00 (C-2′), 102.75 (C-10), 98.30 (C-6), and 93.39 (C-8). Negative ESI mass (m/z): (M-H) - 301 m/z, 284 m/z, 271 m/z, 255 m/z, and 151 m/z.

4.2. Cytotoxicity Activities

The cytotoxic activities of isolated flavonoids and the MeOH extract are presented in Table 1. Compound 2 demonstrated significant cytotoxic activity against PC3 ($P < 0.01$), while compound 3 exhibited significant cytotoxic activity against MCF-7 and HeLa ($P < 0.01$), compared to other samples. Additionally, compound 3 and the MeOH extract exhibited the highest cytotoxic activity on HUVEC ($P < 0.01$), compared to the other isolated compounds. Several studies have shown the cytotoxic effects of flavonoids, including those isolated from *Allium* plants (6, 7). A noteworthy point in these studies is the lower cytotoxic effects of flavonoids on normal cell lines compared to cancer cells, which may indicate fewer side effects of flavonoids (33). Xiao and Parkin demonstrated the cytotoxic effects of *A. cepa* and its phenolic compounds on liver cancer lines (34).

4.3. Anti-angiogenic Activities

The results of the anti-angiogenesis activities of isolated flavonoids (1 - 3) and the MeOH extract of *A. colchicifolium* bulbs on the CAM model of angiogenesis are shown in Figure 2A and B. The IC_{50} of each compound was considered as the concentration that caused 50% inhibition of angiogenesis in a 100 mm^2 area surrounding each sample disc compared to the negative control disc (distilled water). The MeOH extract (IC_{50} = 4.2 ± 0.25 µg/mL, $P < 0.001$) and compound 3 (5.3 ± 0.3 µg/mL, $P < 0.01$) revealed significant inhibitory effects on neovascularization compared to compounds 1 (IC_{50} = 7.12 ± 0.1 µg/mL) and 2 (IC_{50} = 6 ± 0.21 µg/mL). Quercetin and its derivatives have shown anti-angiogenesis activities in various studies. Tan and co-workers demonstrated that quercetin at 10 nM on the CAM model exhibited anti-angiogenesis by blocking matrix metalloproteinase-2 gene expression (35). Inhibition of protein kinase C (PKC), VEGF, and AKT/mTOR are among other mechanisms of anti-angiogenesis by quercetin derivatives (36-38). Alonso-Castro et al. showed that rutin (compound 1) inhibited angiogenesis at 20 mg/kg by reducing mice VEGF serum levels (39). Additionally, quercetin and 8-methylquercetin-3,5,7,3',4'-pentamethyl ether demonstrated anti-angiogenesis activities at 25 µM through blocking VEGF receptor-2 and angiogenesis cellular signaling pathways (40). In a meta-analysis study, Khater et al. showed that the presence of sugar groups in position 3 has no significant effect on the anti-angiogenic activities of flavonoids, which was also observed in our study (41).

4.4. Molecular Docking

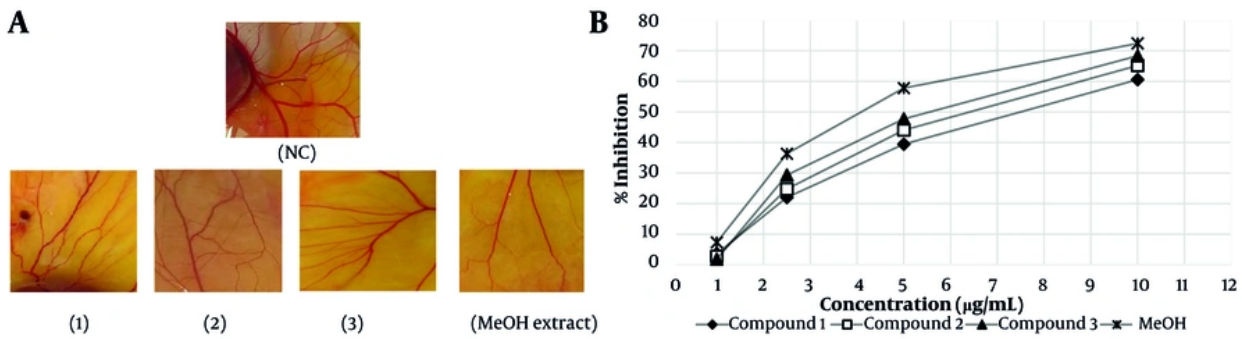

Figure 2. A, anti-angiogenesis activities of isolated compounds (1-3) and the MeOH extract of *Allium colchicifolium* bulbs on the chorioallantoic membrane (CAM) model of angiogenesis at 10 µg/mL; B, percentage of neovascular inhibition of isolated compounds (1-3) and the MeOH extract from *A. colchicifolium* bulbs (abbreviation: NC, negative control).

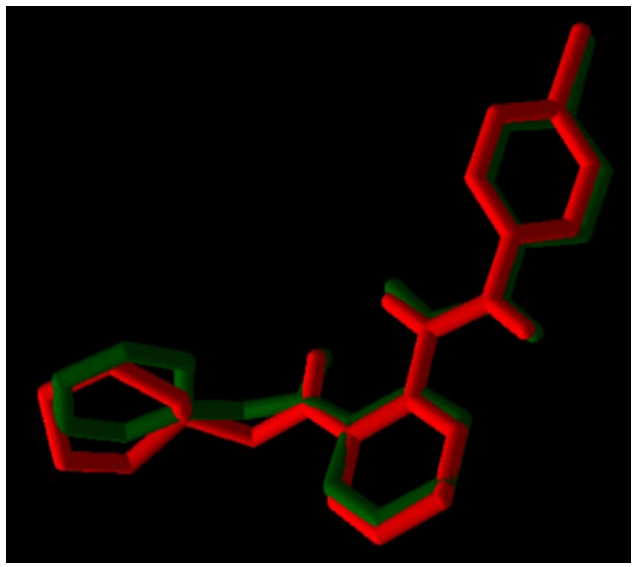

Figure 3. Validation of docking protocol; co-crystallized ligand (8ST): Green; redocked ligand: Red.

For validation of docking, the co-crystallographic ligand (8ST) within VEGF-R1 (PDB ID: 3HNG) was redocked. As shown in Figure 3, 8ST and its redocked structure overlapped well. In the present study, the RMSD value was 0.44, which was within the range of < 2 .0 Å, indicating the accuracy of the docking protocol (42). Binding affinities of compounds on protein targets are shown in Table 2. Compounds 1 (Figure 4) and 3 showed the highest interaction with VEGF-R1 (-9.7 kcal/mol), and compound 3 showed the highest interaction with VEGF-A, C, and D, with binding affinities of -9.4, -6.6, and -7.2 kcal/mol, respectively. The strong interaction of compound 3 with VEGF-R1 and VEGFs can justify the stronger activities of this compound compared to other compounds in the CAM model (Figure 2).

Table 2. Binding Affinity Values Against the Target Proteins

Ligand	VEGF-R1 (3HNG)	VEGF-A (1VPF)	VEGF-B (2C7W)	VEGF-C (2X1X)	VEGF-D (2XV7)
Compound 1	-9.7	-7.5	-7.2	-5.7	-6.2
Compound 2	-8.2	-7.9	-7.0	-5.8	-6.1
Compound 3	-9.7	-9.4	-7.0	-6.6	-7.2

Abbreviation: VEGF, vascular endothelial growth factor receptor.

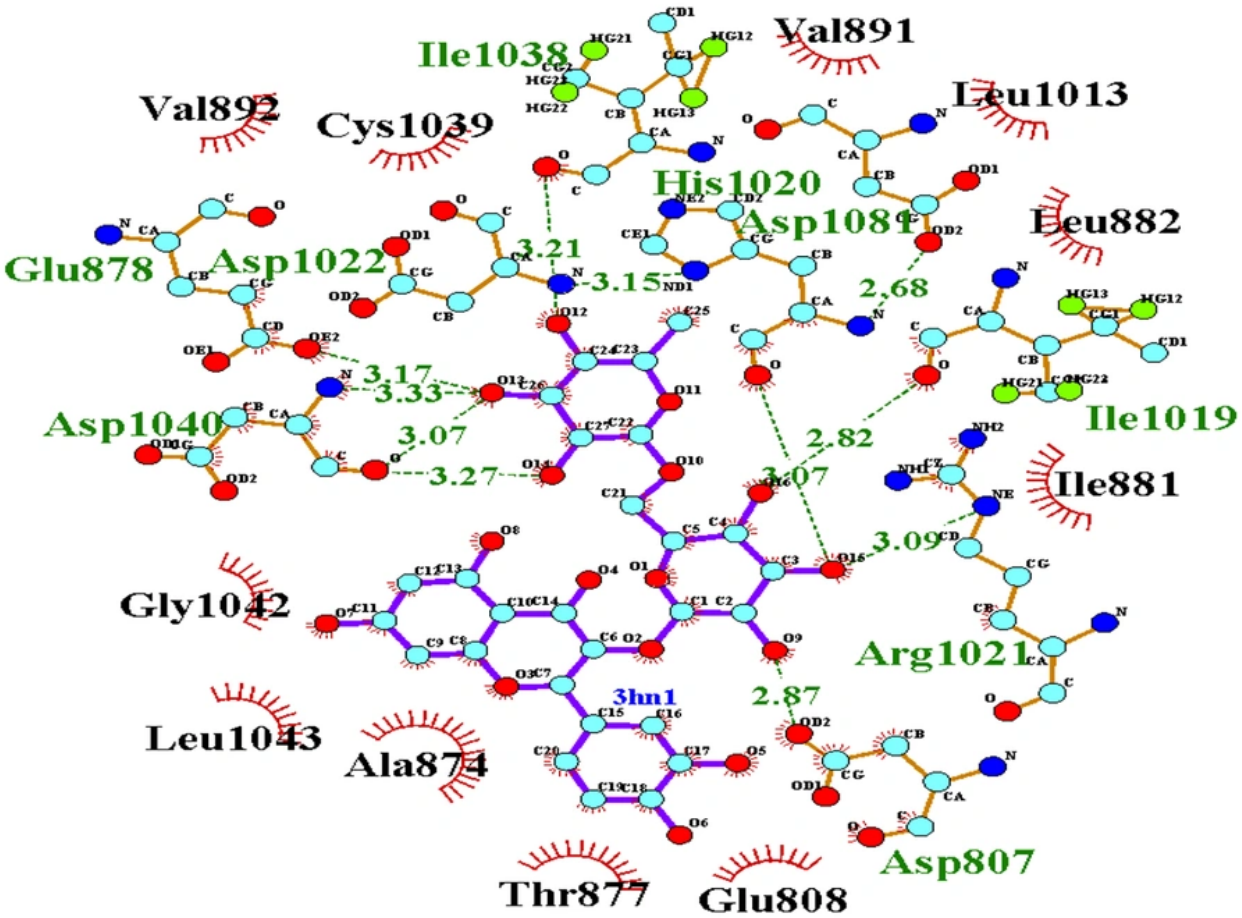

Figure 4. 2D Interaction of compound 1 with vascular endothelial growth factor (VEGF)-R1: Compound 1 formed hydrogen bonds with Asp1040 (3.27, 3.07, and 3.33 Å), Glu878 (3.17 Å), and Ile1038 (3.21 Å) and hydrophobically interacted with Leu882 and Cys1039.

4.5. Absorption, Distribution, Metabolism, Excretion, and Toxicity Analysis

The Lipinski Ro5 is commonly used for evaluating drug-likeness, which states that absorption or permeation is more likely for compounds possessing a molecular weight (MW) < 500, lipophilicity (LogP) < 5, a number of hydrogen bond acceptors (HBA) (sum of Ns and Os) < 10, and a number of hydrogen bond donors (HBD) (sum of OHs and NHs) < 5. At most one violation is acceptable (43). Compound 3, based on Ro5, is drug-like (Table 3). The topological polar surface area (TPSA)

Table 3. Drug-Likeness Prediction Through ADMETlab

Ligand	MW (≤ 500)	HBA (≤ 10)	HBD (≤ 5)	LogP	TPSA (Å^2)	Lipinski Rule
Compound 1	610.150	16	10	-0.038	269.430	Rejected
Compound 2	478.110	12	7	0.559	199.510	Rejected
Compound 3	300.070	5	3	3.678	90.900	Accepted

Abbreviations: MW, molecular weight; HBA, hydrogen bond acceptors; HBD, hydrogen bond donors; TPSA, topological polar surface area.

Table 4. Pharmacokinetics and Toxicity Prediction by AdmetSAR

Ligand	BBB Permeant	GI Absorption	P-gp Substrate	CYP2C9 Inhibitor	hERG Inhibition	Carcinogens	AMES Toxicity
Compound 1	BBB-	HIA$^+$	Substrate	Non-inhibitor	Weak inhibitor	Non-carcinogenic	Non-AMES toxic
Compound 2	BBB-	HIA$^+$	Substrate	Non-inhibitor	Weak inhibitor	Non-carcinogenic	Non-AMES toxic
Compound 3	BBB-	HIA$^+$	Substrate	Inhibitor	Weak inhibitor	Non-carcinogenic	AMES toxic

Abbreviations: GI, gastrointestinal; HIA, human intestinal absorption; BBB, blood-brain barrier; P-gp, P-glycoprotein; CYP, cytochrome P450; hERG, human ether-a-go-go-related gene.

values for compound 3 were less than 140 Å^2, indicating proper permeability in the cell membrane (44). In terms of pharmacokinetic properties, compounds 1, 2, and 3 failed blood-brain barrier (BBB) permeation (Table 4). All compounds are human intestinal absorption (HIA$^+$) and P-glycoprotein (P-gp) substrates. Additionally, only compound 3 may be an inhibitor of CYP2C9. All these compounds are non-carcinogenic and are weak inhibitors of hERG. The hERG encodes a voltage-gated potassium channel in cardiac myocytes that plays an important role in action potential membrane repolarization, and hERG channel blockade is associated with long QT syndrome (45). Overall, compound 3 exhibited better ADMET profiles compared to others, although in terms of mutagenicity (46), compound 3 showed positive AMES toxicity.

4.6. Conclusions

In this study, two glycosylated flavonoids, including rutin (compound 1) and isorhamnetin 3-O-glucoside (compound 2), and one aglycone, including quercetin (compound 3), were isolated by CC methods and identified from *A. colchicifolium* bulbs for the first time. Additionally, the cytotoxic and anti-angiogenic activities of the MeOH extract of the *A. colchicifolium* bulbs and its isolated flavonoids were investigated using MTT and CAM models, respectively. The results of the present study demonstrated the notable cytotoxic and anti-angiogenic activities of the MeOH extract. Furthermore, compound 3, as an aglycone flavonoid, exhibited significant anti-angiogenesis activities with an IC_{50} of 5.3 ± 0.3 µg/mL and cytotoxic effects with an IC_{50} ≤ 3 µg/mL against PC3 and MCF, which is consistent with other studies (40). Additionally, a docking study assessed the interaction of the compounds with VEGF, one of the most critical mediators of angiogenesis induction (47, 48), and compound 3 exhibited the strongest interaction. The anti-cancer effects of edible plants and their phytochemicals, including A. plants and their flavonoids, as reliable and available sources, have always attracted the attention of researchers to discover effective molecules for the treatment of various types of malignancy (40, 41). On the other hand, the crucial limitation of using flavonoids for the treatment of various diseases, including malignancies, is their low bioavailability. The use of new drug delivery techniques to increase their bioavailability offers a potential solution. Furthermore, experimental studies have shown that flavonoids can have synergistic effects with chemotherapy drugs. This synergy could enable a reduction in the dosage of chemotherapy drugs with high side effects, such as doxorubicin, in patients (49). According to our results, the MeOH extract of *A. colchicifolium* can be a rich source of polyphenolic compounds, including anticancer flavonoids. Our previous study on the leaves of this plant also showed the presence of polyphenolic compounds with antibacterial and biofilm activities. Therefore,

considering the aforementioned biological effects, *A. colchicifolium* can be introduced as a promising candidate for drug molecule discovery (16). Therefore, comprehensive clinical trials are suggested to assess their bioavailability and efficacy.

Acknowledgements

The authors are grateful to the Pharmaceutical Sciences Research Center of Isfahan University of Medical Sciences for their valuable assistance.

Supplementary Material

Supplementary material(s) is available here [To read supplementary materials, please refer to the journal website and open PDF/HTML].

Footnotes

Authors' Contribution: Study concept and design: M. B. M., M. M., K. M., and S. M. G.; Analysis and interpretation of data: M. B. M., G. R. B., and S. M. G.; Drafting of the manuscript: M. B. M.; Critical revision of the manuscript for important intellectual content: M. M., K. M., and S. M. G.; Statistical analysis: M. B. M. and S. M. G.

Conflict of Interests Statement: The authors declare that there is no conflict of interest.

Data Availability: The dataset presented in the study is available on request from the corresponding author during submission or after publication.

Ethical Approval: IR.KUMS.REC.1400.552 .

Funding/Support: The present study received no funding/support.

References

1. Simin N, Orcic D, Cetojevic-Simin D, Mimica-Dukic N, Anackov G, Beara I, et al. Phenolic profile, antioxidant, anti-inflammatory and cytotoxic activities of small yellow onion (Allium flavum L. subsp. flavum, Alliaceae). *LWT - Food Sci Technol*. 2013;**54**(1):139-46. https://doi.org/10.1016/j.lwt.2013.05.023.
2. Seyfi P, Mostafaie A, Mansouri K, Arshadi D, Mohammadi-Motlagh HR, Kiani A. In vitro and in vivo anti-angiogenesis effect of shallot (Allium ascalonicum): a heat-stable and flavonoid-rich fraction of shallot extract potently inhibits angiogenesis. *Toxicol In Vitro*. 2010;**24**(6):1655-61. [PubMed ID: 20570718]. https://doi.org/10.1016/j.tiv.2010.05.022.
3. Veiga AA, Irioda AC, Mogharbel BF, Bonatto SJR, Souza LM. Quercetin-Rich Extracts from Onions (Allium cepa) Play Potent Cytotoxicity on Adrenocortical Carcinoma Cell Lines, and Quercetin Induces Important Anticancer Properties. *Pharmaceuticals (Basel)*. 2022;**15**(6). [PubMed ID: 35745673]. [PubMed Central ID: PMC9228762]. https://doi.org/10.3390/ph15060754.
4. Tigu AB, Moldovan CS, Toma VA, Farcas AD, Mot AC, Jurj A, et al. Phytochemical Analysis and In Vitro Effects of Allium fistulosum L. and Allium sativum L. Extracts on Human Normal and Tumor Cell Lines: A Comparative Study. *Molecules*. 2021;**26**(3). [PubMed ID: 33499159]. [PubMed Central ID: PMC7866094]. https://doi.org/10.3390/molecules26030574.
5. Lanzotti V, Scala F, Bonanomi G. Compounds from Allium species with cytotoxic and antimicrobial activity. *Phytochemistry Rev*. 2014;**13**(4):769-91. https://doi.org/10.1007/s11101-014-9366-0.
6. Asemani Y, Zamani N, Bayat M, Amirghofran Z. Allium vegetables for possible future of cancer treatment. *Phytother Res*. 2019;**33**(12):3019-39. [PubMed ID: 31464060]. https://doi.org/10.1002/ptr.6490.
7. Kothari D, Lee WD, Kim SK. Allium Flavonols: Health Benefits, Molecular Targets, and Bioavailability. *Antioxidants (Basel)*. 2020;**9**(9). [PubMed ID: 32961762]. [PubMed Central ID: PMC7555649]. https://doi.org/10.3390/antiox9090888.
8. Abdel-Hady H, El-Sayed MM, Abdel-Gawad MM, El-Wakil EA, Abdel-Hameed ESS, Abdel-Lateef EES. LC-ESI-MS analysis, antitumor and antioxidant activities of methanolic extract of Egyptian Allium kurrat. *J Appl Pharm Sci*. 2018;**8**(7):85-92. https://doi.org/10.7324/japs.2018.8714.
9. Mostafaie A, Arshadi D, Mansouri K, Khodarahmi R, Seyfi P, Shakiba Y. In vitro anti-angiogenic activity of persian shallot (Allium Hirtifolium) extract is mediated through inhibition of endothelial cell proliferation/migration and down-regulation of VEGF and MMP expression. *J Rep Pharm Sci*. 2014;**3**(1). https://doi.org/10.4103/2322-1232.222549.
10. Aleksandar P, Dragana MC, Nebojsa J, Biljana N, Natasa S, Branka V, et al. Wild edible onions - Allium flavum and Allium carinatum - successfully prevent adverse effects of chemotherapeutic drug doxorubicin. *Biomed Pharmacother*. 2019;**109**:2482-91. [PubMed ID: 30551509]. https://doi.org/10.1016/j.biopha.2018.11.106.
11. Ponte LGS, Pavan ICB, Mancini MCS, da Silva LGS, Morelli AP, Severino MB, et al. The Hallmarks of Flavonoids in Cancer. *Molecules*. 2021;**26**(7). [PubMed ID: 33918290]. [PubMed Central ID: PMC8038160]. https://doi.org/10.3390/molecules26072029.
12. Abdi F, Arkan E, Eidizadeh M, Valipour E, Naseriyeh T, Gamizgy YH, et al. The possibility of angiogenesis inhibition in cutaneous melanoma by bevacizumab-loaded lipid-chitosan nanoparticles. *Drug Deliv Transl Res*. 2023;**13**(2):568-79. [PubMed ID: 36058987]. https://doi.org/10.1007/s13346-022-01215-5.
13. Jahani M, Azadbakht M, Rasouli H, Yarani R, Rezazadeh D, Salari N, et al. L-arginine/5-fluorouracil combination treatment approaches cells selectively: Rescuing endothelial cells while killing MDA-MB-468 breast cancer cells. *Food Chem Toxicol*. 2019;**123**:399-411. [PubMed ID: 30423404]. https://doi.org/10.1016/j.fct.2018.11.018.
14. Bratty MA. Spectroscopic and molecular docking studies for characterizing binding mechanism and conformational changes of human serum albumin upon interaction with Telmisartan. *Saudi Pharm J*. 2020;**28**(6):729-36. [PubMed ID: 32550805]. [PubMed Central ID: PMC7292872]. https://doi.org/10.1016/j.jsps.2020.04.015.

15. Duchowicz PR, Bacelo DE, Fioressi SE, Palermo V, Ibezim NE, Romanelli GP. QSAR studies of indoyl aryl sulfides and sulfones as reverse transcriptase inhibitors. *Med Chem Res*. 2017;**27**(2):420-8. https://doi.org/10.1007/s00044-017-2069-5.
16. Majnooni MB, Ghanadian SM, Mojarrab M, Bahrami G, Mansouri K, Mirzaei A, et al. Antibacterial, Antibiofilm, Antiswarming, and Antioxidant Activities of Flavonoids Isolated from Allium colchicifolium Leaves. *J Food Biochem*. 2023;**2023**:1-14. https://doi.org/10.1155/2023/5521661.
17. Fattorusso E, Lanzotti V, Taglialatela-Scafati O, Cicala C. The flavonoids of leek, Allium porrum. *Phytochemistry*. 2001;**57**(4):565-9. [PubMed ID: 11394858]. https://doi.org/10.1016/s0031-9422(01)00039-5.
18. Mousavi SH, Motaez M, Zamiri-Akhlaghi A, Emami SA, Tayarani-Najaran Z. In-vitro Evaluation of Cytotoxic and Apoptogenic Properties of Sophora Pachycarpa. *Iran J Pharm Res*. 2014;**13**(2):665-73. [PubMed ID: 25237363]. [PubMed Central ID: PMC4157043].
19. Fathian Kolahkaj F, Derakhshandeh K, Khaleseh F, Azandaryani AH, Mansouri K, Khazaei M. Active targeting carrier for breast cancer treatment: Monoclonal antibody conjugated epirubicin loaded nanoparticle. *J Drug Delivery Sci Technol*. 2019;**53**. https://doi.org/10.1016/j.jddst.2019.101136.
20. Shahik SM, Salauddin A, Hossain MS, Noyon SH, Moin AT, Mizan S, et al. Screening of novel alkaloid inhibitors for vascular endothelial growth factor in cancer cells: an integrated computational approach. *Genomics Inform*. 2021;**19**(1). e6. [PubMed ID: 33840170]. [PubMed Central ID: PMC8042301]. https://doi.org/10.5808/gi.20068.
21. Leppanen VM, Prota AE, Jeltsch M, Anisimov A, Kalkkinen N, Strandin T, et al. Structural determinants of growth factor binding and specificity by VEGF receptor 2. *Proc Natl Acad Sci U S A*. 2010;**107**(6):2425-30. [PubMed ID: 20145116]. [PubMed Central ID: PMC2823880]. https://doi.org/10.1073/pnas.0914318107.
22. Soudani W, Hadjadj-Aoul FZ, Bouachrine M, Zaki H. Molecular docking of potential cytotoxic alkylating carmustine derivatives 2-chloroethylnitrososulfamides analogues of 2-chloroethylnitrosoureas. *J Biomol Struct Dyn*. 2021;**39**(12):4256-69. [PubMed ID: 32490742]. https://doi.org/10.1080/07391102.2020.1776638.
23. Laskowski RA, Swindells MB. LigPlot+: multiple ligand-protein interaction diagrams for drug discovery. *J Chem Inf Model*. 2011;**51**(10):2778-86. [PubMed ID: 21919503]. https://doi.org/10.1021/ci200227u.
24. Moroy G, Martiny VY, Vayer P, Villoutreix BO, Miteva MA. Toward in silico structure-based ADMET prediction in drug discovery. *Drug Discov Today*. 2012;**17**(1-2):44-55. [PubMed ID: 22056716]. https://doi.org/10.1016/j.drudis.2011.10.023.
25. Lipinski CA, Lombardo F, Dominy BW, Feeney PJ. Experimental and computational approaches to estimate solubility and permeability in drug discovery and development settings. *Advanced Drug Delivery Rev*. 2012;**64**:4-17. https://doi.org/10.1016/j.addr.2012.09.019.
26. Kachlicki P, Piasecka A, Stobiecki M, Marczak L. Structural Characterization of Flavonoid Glycoconjugates and Their Derivatives with Mass Spectrometric Techniques. *Molecules*. 2016;**21**(11). [PubMed ID: 27834838]. [PubMed Central ID: PMC6273528]. https://doi.org/10.3390/molecules21111494.
27. Cuyckens F, Claeys M. Mass spectrometry in the structural analysis of flavonoids. *J Mass Spectrom*. 2004;**39**(1):1-15. [PubMed ID: 14760608]. https://doi.org/10.1002/jms.585.
28. El Shabrawy MO, Hosni HA, El Garf IA, Marzouk MM, Kawashty SA, Saleh NA. Flavonoids from Allium myrianthum Boiss. *Biochemical Syst Ecol*. 2014;**56**:125-8. https://doi.org/10.1016/j.bse.2014.05.015.
29. Slimestad R, Fossen T, Vagen IM. Onions: a source of unique dietary flavonoids. *J Agric Food Chem*. 2007;**55**(25):10067-80. [PubMed ID: 17997520]. https://doi.org/10.1021/jf0712503.
30. Wang DM, Pu WJ, Wang YH, Zhang YJ, Wang SS. A new isorhamnetin glycoside and other phenolic compounds from Callianthemum taipaicum. *Molecules*. 2012;**17**(4):4595-603. [PubMed ID: 22510608]. [PubMed Central ID: PMC6268643]. https://doi.org/10.3390/molecules17044595.
31. Carotenuto A, Fattorusso E, Lanzotti V, Magno S, De Feo V, Cicala C. The flavonoids of Allium neapolitanum. *Phytochemistry*. 1997;**44**(5):949-57. [PubMed ID: 9115694]. https://doi.org/10.1016/s0031-9422(96)00663-2.
32. Nakane R, Iwashina T. Flavonol Glycosides from the Leaves of Allium Macrostemon. *Natural Product Communications*. 2015;**10**(8). https://doi.org/10.1177/1934578x1501000817.
33. Šmejkal K. Cytotoxic potential of C-prenylated flavonoids. *Phytochemistry Rev*. 2013;**13**(1):245-75. https://doi.org/10.1007/s11101-013-9308-2.
34. Xiao H, Parkin KL. Isolation and identification of potential cancer chemopreventive agents from methanolic extracts of green onion (Allium cepa). *Phytochemistry*. 2007;**68**(7):1059-67. [PubMed ID: 17350659]. https://doi.org/10.1016/j.phytochem.2007.01.021.
35. Tan WF, Lin LP, Li MH, Zhang YX, Tong YG, Xiao D, et al. Quercetin, a dietary-derived flavonoid, possesses antiangiogenic potential. *Eur J Pharmacol*. 2003;**459**(2-3):255-62. [PubMed ID: 12524154]. https://doi.org/10.1016/s0014-2999(02)02848-0.
36. Igura K, Ohta T, Kuroda Y, Kaji K. Resveratrol and quercetin inhibit angiogenesis in vitro. *Cancer Lett*. 2001;**171**(1):11-6. [PubMed ID: 11485823]. https://doi.org/10.1016/s0304-3835(01)00443-8.
37. Pratheeshkumar P, Budhraja A, Son YO, Wang X, Zhang Z, Ding S, et al. Quercetin inhibits angiogenesis mediated human prostate tumor growth by targeting VEGFR- 2 regulated AKT/mTOR/P70S6K signaling pathways. *PLoS One*. 2012;**7**(10). e47516. [PubMed ID: 23094058]. [PubMed Central ID: PMC3475699]. https://doi.org/10.1371/journal.pone.0047516.
38. Schindler R, Mentlein R. Flavonoids and vitamin E reduce the release of the angiogenic peptide vascular endothelial growth factor from human tumor cells. *J Nutr*. 2006;**136**(6):1477-82. [PubMed ID: 16702307]. https://doi.org/10.1093/jn/136.6.1477.
39. Alonso-Castro AJ, Dominguez F, Garcia-Carranca A. Rutin exerts antitumor effects on nude mice bearing SW480 tumor. *Arch Med Res*. 2013;**44**(5):346-51. [PubMed ID: 23867787]. https://doi.org/10.1016/j.arcmed.2013.06.002.
40. Lupo G, Cambria MT, Olivieri M, Rocco C, Caporarello N, Longo A, et al. Anti-angiogenic effect of quercetin and its 8-methyl pentamethyl ether derivative in human microvascular endothelial cells. *J Cell Mol Med*. 2019;**23**(10):6565-77. [PubMed ID: 31369203]. [PubMed Central ID: PMC6787496]. https://doi.org/10.1111/jcmm.14455.
41. Khater M, Greco F, Osborn HMI. Antiangiogenic Activity of Flavonoids: A Systematic Review and Meta-Analysis. *Molecules*. 2020;**25**(20). [PubMed ID: 33066630]. [PubMed Central ID: PMC7594036]. https://doi.org/10.3390/molecules25204712.
42. Azam F, Prasad MV, Thangavel N, Ali HI. Molecular docking studies of 1-(substituted phenyl)-3-(naphtha [1, 2-d] thiazol-2-yl) urea/thiourea derivatives with human adenosine A(2A) receptor. *Bioinformation*. 2011;**6**(9):330-4. [PubMed ID: 21814389]. [PubMed Central ID: PMC3143394]. https://doi.org/10.6026/97320630006330.

43. Lipinski CA, Lombardo F, Dominy BW, Feeney PJ. Experimental and computational approaches to estimate solubility and permeability in drug discovery and development settings. *Adv Drug Delivery Rev*. 1997;**23**(1-3):3-25. https://doi.org/10.1016/s0169-409x(96)00423-1.
44. Alsaffar RM, Ali A, Rashid SM, Ahmad SB, Alkholifi FK, Kawoosa MS, et al. Zerumbone Protects Rats from Collagen-Induced Arthritis by Inhibiting Oxidative Outbursts and Inflammatory Cytokine Levels. *ACS Omega*. 2023;**8**(3):2982-91. [PubMed ID: 36713739]. [PubMed Central ID: PMC9878628]. https://doi.org/10.1021/acsomega.2c05749.
45. Feng H, Wei GW. Virtual screening of DrugBank database for hERG blockers using topological Laplacian-assisted AI models. *Comput Biol Med*. 2023;**153**:106491. [PubMed ID: 36599209]. [PubMed Central ID: PMC10120853]. https://doi.org/10.1016/j.compbiomed.2022.106491.
46. Al-Jumaili MHA, Siddique F, Abul Qais F, Hashem HE, Chtita S, Rani A, et al. Analysis and prediction pathways of natural products and their cytotoxicity against HeLa cell line protein using docking, molecular dynamics and ADMET. *J Biomol Struct Dyn*. 2023;**41**(3):765-77. [PubMed ID: 34861809]. https://doi.org/10.1080/07391102.2021.2011785.
47. Lee C, Kim MJ, Kumar A, Lee HW, Yang Y, Kim Y. Vascular endothelial growth factor signaling in health and disease: from molecular mechanisms to therapeutic perspectives. *Signal Transduct Target Ther*. 2025;**10**(1):170. [PubMed ID: 40383803]. [PubMed Central ID: PMC12086256]. https://doi.org/10.1038/s41392-025-02249-0.
48. Li Y, Li Y, Qian Z, Ryu B, Kim S. Suppression of vascular endothelial growth factor (VEGF) induced angiogenic responses by fucodiphloroethol G. *Process Biochem*. 2011;**46**(5):1095-103. https://doi.org/10.1016/j.procbio.2011.01.035.
49. Zeinali M, Abbaspour-Ravasjani S, Ghorbani M, Babazadeh A, Soltanfam T, Santos AC, et al. Nanovehicles for co-delivery of anticancer agents. *Drug Discov Today*. 2020;**25**(8):1416-30. [PubMed ID: 32622880]. https://doi.org/10.1016/j.drudis.2020.06.027.